

# The Universal Equilibrium of CDM Halos: Making Tracks on the Cosmic Virial Plane <sup>\*</sup>

Ilian T. Iliev<sup>1</sup> and Paul R. Shapiro<sup>2</sup>

<sup>1</sup> Osservatorio Astrofisico di Arcetri, Largo Enrico Fermi 5, 50125 Firenze, Italy

<sup>2</sup> Department of Astronomy, University of Texas, Austin, 78712, USA

**Abstract.** Dark-matter halos are the scaffolding around which galaxies and clusters are built. They form when the gravitational instability of primordial density fluctuations causes regions which are denser than average to slow their cosmic expansion, recollapse, and virialize. Objects as different in size and mass as dwarf spheroidal galaxies and galaxy clusters are predicted by the CDM model to have halos with a universal, self-similar equilibrium structure whose parameters are determined by the halo’s total mass and collapse redshift. These latter two are statistically correlated, however, since halos of the same mass form on average at the same epoch, with small-mass objects forming first and then merging hierarchically. The structural properties of dark-matter dominated halos of different masses, therefore, should reflect this statistical correlation, an imprint of the statistical properties of the primordial density fluctuations which formed them. Current data reveal these correlations, providing a fundamental test of the CDM model which probes the shape of the power spectrum of primordial density fluctuations and the cosmological background parameters.

## 1 The Truncated Isothermal Sphere (TIS) Model

We have developed an analytical model for the postcollapse equilibrium structure of virialized objects which condense out of a cosmological background universe, either matter-dominated or flat with a cosmological constant [23,8]. The model is based upon the assumption that cosmological halos form from the collapse and virialization of “top-hat” density perturbations and are spherical, isotropic, and isothermal. This leads to a unique, nonsingular TIS, a particular solution of the Lane-Emden equation (suitably modified when  $\Lambda \neq 0$ ). The size  $r_t$  and velocity dispersion  $\sigma_V$  are unique functions of the mass and redshift of formation of the object for a given background universe. Our TIS density profile flattens to a constant central value,  $\rho_0$ , which is roughly proportional to the critical density of the universe at the epoch of collapse, with a small core radius  $r_0 \approx r_t/30$  (where  $\sigma_V^2 = 4\pi G\rho_0 r_0^2$  and  $r_0 \equiv r_{\text{King}}/3$ , for the “King radius”  $r_{\text{King}}$ , defined by [1], p. 228). The density profiles for gas and dark matter are assumed to be the same (no bias), with gas temperature  $T = \mu m_p \sigma_V^2 / k_B$ .

These TIS results differ from those of the more familiar approximations in which the virialized sphere resulting from a top-hat perturbation is assumed to be either the standard uniform sphere (SUS) or else a singular isothermal

---

<sup>\*</sup> to appear in “The Mass of Galaxies at Low and High Redshift” (ESO Astrophysics Symposia), eds. R. Bender & A. Renzini, Springer-Verlag, Heidelberg, in press (2002)

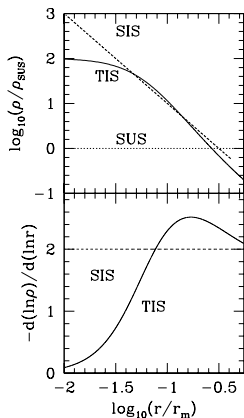


**Fig. 1.** (top) Density profile of TIS in a matter-dominated universe. Radius  $r$  is in units of  $r_m$  - the top-hat radius at maximum expansion. Density  $\rho$  is in terms of the density  $\rho_{\text{SUS}}$  of the SUS approximation for the virialized, post-collapse top-hat. (bottom) Logarithmic slope of density profile.

sphere (SIS). We summarize their comparison in Fig. 1 and Table 1, where  $\eta$  is the final radius of the virialized sphere in units of the top-hat radius  $r_m$  at maximum expansion (i.e.  $\eta_{\text{SUS}} = 0.5$ ),  $\rho_t \equiv \rho(r_t)$ ,  $\langle \rho \rangle$  is the average density of the virialized spheres,  $\Delta_c = \langle \rho \rangle / \rho_{\text{crit}}(t_{\text{coll}})$ , and  $K/|W|$  is the ratio of total kinetic (i.e. thermal) to gravitational potential energy of the spheres.

## 2 TIS Model vs. Numerical CDM Simulations

The TIS model reproduces many of the average properties of the halos in numerical CDM simulations quite well, suggesting that it is a useful approximation for the halos which result from more realistic initial conditions:

(1) The TIS mass profile agrees well with the fit to N-body simulations by [18] (“NFW”) (i.e. fractional deviation of  $\sim 20\%$  or less) at all radii outside of a few TIS core radii (i.e. outside King radius or so), for NFW concentration parameters  $4 \leq c_{\text{NFW}} \leq 7$  (Fig. 2). The flat density core of the TIS halo differs from the singular cusp of the NFW profile at small radii, but this involves only a small fraction of the halo mass, thus not affecting their good agreement outside the core. As a result, the TIS central density  $\rho_0$  can be used to characterize the core density of cosmological halos, even if the latter have singular profiles like that of NFW, as long as we interpret  $\rho_0$ , in that case, as an average over the innermost region.

(2) The TIS halo model predicts the internal structure of X-ray clusters found by gas-dynamical/N-body simulations of cluster formation in the CDM model. Our TIS model predictions, for example, agree astonishingly well with the

Table 1

	SUS	SIS	TIS <sup>a</sup>
$\eta/\eta_{\text{SUS}}$	1	0.833	1.11;1.07
$T/T_{\text{SUS}}$	1	3	2.16;2.19
$\rho_0/\rho_t$	1	$\infty$	514;530
$\langle \rho \rangle/\rho_t$	1	3	3.73;3.68
$r_t/r_0$	- NA -	$\infty$	29.4;30.04
$\Delta_c/\Delta_{c,\text{SUS}}$	1	1.728	0.735;0.774
$K/ W $	0.5	0.75	0.683;0.690

<sup>a</sup> The two values refer to flat universe with  $\Lambda = 0$  (left value) and  $\Omega_0 = 0.3$ ,  $\lambda_0 = 0.7$  (right value).

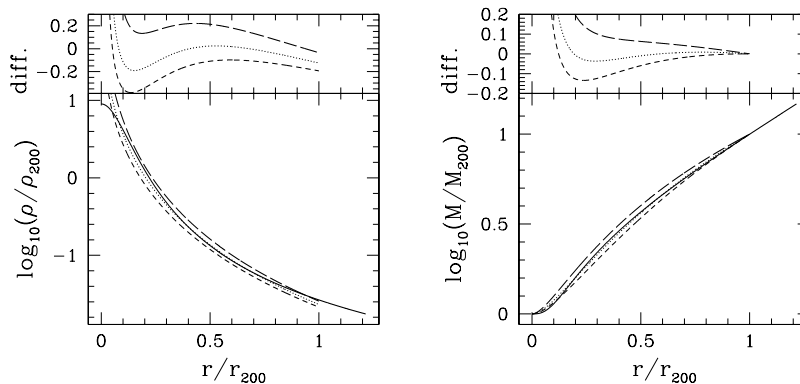


**Fig. 2.** Profiles of density (left) and integrated mass (right), for TIS (solid) and NFW with  $c_{\text{NFW}} = 4$  (short-dashed), 5 (dotted) and 7 (long-dashed) with same  $(r_{200}, M_{200})$ .

mass-temperature and radius-temperature virial relations and integrated mass profiles derived empirically from the simulations of cluster formation by [4,16] (EMN). Apparently, these simulation results are not sensitive to the discrepancy between our prediction of a small, finite density core and the N-body predictions of a density cusp for clusters in CDM. Let  $X$  be the average overdensity inside radius  $r$  (in units of the cosmic mean density)  $X \equiv \langle \rho(r) \rangle / \rho_b$ . The radius-temperature virial relation is defined as  $r_X \equiv r_{10}(X)(T/10 \text{ keV})^{1/2} \text{ Mpc}$ , and the mass-temperature virial relation by  $M_X \equiv M_{10}(X)(T/10 \text{ keV})^{1/2} h^{-1} 10^{15} M_\odot$ . A comparison between our predictions of  $r_{10}(X)$  and the results of EMN is given in Fig. 3. EMN obtain  $M_{10}(500) = 1.11 \pm 0.16$  and  $M_{10}(200) = 1.45$ , while our TIS solution yields  $M_{10}(500) = 1.11$  and  $M_{10}(200) = 1.55$ .

(3) The TIS halo model also successfully reproduces the mass - velocity dispersion relation for clusters in CDM N-body simulations and its dependence on redshift for different background cosmologies. N-body simulation of the Hubble volume  $[(1000 \text{ Mpc})^3]$  by the Virgo Consortium (reported by Evrard at the U. of Victoria meeting, August 2000) yields the following empirical relation:

$$\sigma_V = (1080 \pm 65) [h(z)M_{200}/10^{15}M_\odot]^{0.33} \text{ km/s}, \quad (1)$$

where  $M_{200}$  is the mass within a sphere with average density 200 times the cosmic mean density, and  $h(z) = h_0 \sqrt{\Omega_0(1+z)^3 + \lambda_0}$  is the redshift-dependent Hubble constant. Our TIS model predicts:

$$\sigma_V = 1103 [h(z)M_{200}/10^{15}M_\odot]^{1/3} \text{ km/s}. \quad (2)$$

(4) The TIS model successfully predicts the average virial ratio,  $K/|W|$ , of halos in CDM simulations. An equivalent TIS quantity,  $GM_{200}/(r_{200}\sigma_V^2) = 2.176$ , is plotted for dwarf galaxy minihalos at  $z = 9$  in Fig. 3(b), from [20], showing good agreement between TIS and N-body halo results. A similar plot,

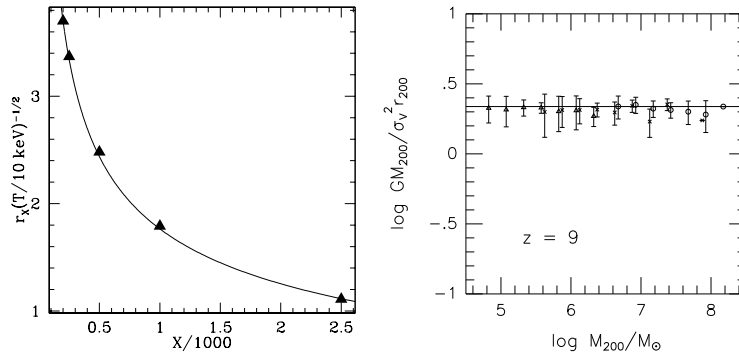


**Fig. 3.** (a) (left) (triangles) Cluster radius-temperature virial relation for CDM simulation results (at  $z = 0$ ) as fit by EMN and as predicted by TIS (solid curve). (b)  $GM_{200}/(\sigma_v^2 r_{200})$  vs. mass for halos from N-body simulations [with  $1\sigma$  error bars]. Horizontal line is analytical prediction of TIS model.

but of  $K/|W|$  for such halos, was shown by [10] based upon N-body simulations, in which the average  $K/|W|$  is close to 0.7, as predicted by the TIS model (Table 1). Those authors were apparently unaware of this TIS prediction since they compared their results with the SUS value of  $K/|W|$ , 0.5, and interpreted the discrepancy incorrectly as an indication that their halos were not in equilibrium.

### 3 TIS Model vs. Observed Halos

(1) The TIS profile matches the observed mass profiles of dark-matter-dominated dwarf galaxies [7]. The observed rotation curves of dwarf galaxies are well fit by a density profile with a finite density core given by

$$\rho(r) = \frac{\rho_{0,B}}{(r/r_c + 1)(r^2/r_c^2 + 1)} \quad (3)$$

[2]. The TIS model gives a nearly perfect fit to this profile (Fig. 4(a)), with best fit parameters  $\rho_{0,B}/\rho_{0,TIS} = 1.216$ ,  $r_c/r_{0,TIS} = 3.134$ . This best-fit TIS profile correctly predicts  $v_{\max}$ , the maximum rotation velocity, and the radius,  $r_{\max}$ , at which it occurs in the Burkert profile:  $r_{\max,B}/r_{\max,TIS} = 1.13$ , and  $v_{\max,B}/v_{\max,TIS} = 1.01$ .

(2) The TIS halo model can explain the mass profile with a flat density core measured by [24] for cluster CL 0024+1654 at  $z = 0.39$ , using the strong gravitational lensing of background galaxies by the cluster to infer the cluster mass distribution [21]. The TIS model not only provides a good fit to the projected surface mass density distribution of this cluster within the arcs (Fig. 4b), but also predicts the overall mass, and a cluster velocity dispersion in close agreement with the value  $\sigma_v = 1150$  km/s measured by [3].

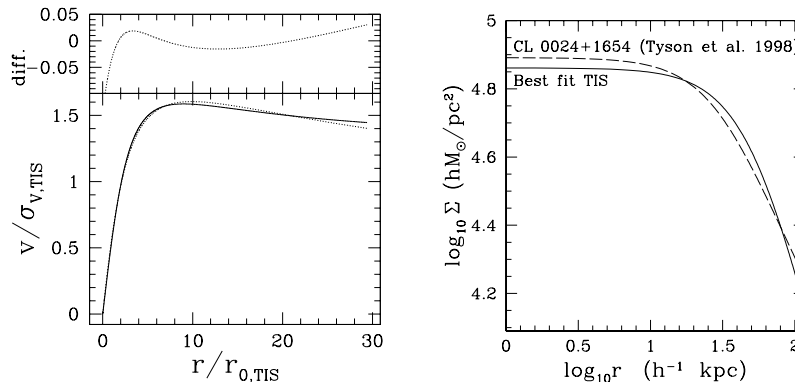


**Fig. 4.** (a) (left) Rotation Curve Fit. Solid line = Best fit TIS; Dashed line = Burkert profile (b) (right) Projected surface density of cluster CL 0024+1654 inferred from lensing measurements, together with the best-fit TIS model.

## 4 Making Tracks on the Cosmic Virial Plane

The TIS model yields  $(\rho_0, \sigma_V, r_t, r_0)$  uniquely as functions of  $(M, z_{\text{coll}})$ . This defines a “cosmic virial plane” in  $(\rho_0, r_0, \sigma_V)$ -space and determines halo size, mass, and collapse redshift for each point on the plane. In hierarchical clustering models like CDM,  $M$  is statistically correlated with  $z_{\text{coll}}$ . This determines the distribution of points on the cosmic virial plane. We can combine the TIS model with the Press-Schechter (PS) approximation for  $z_{\text{coll}}(M)$  – typical collapse epoch for halo of mass  $M$  – to predict correlations of observed halo properties.

(1) The combined (TIS+PS) model explains the observed  $v_{\text{max}} - r_{\text{max}}$  correlation of dwarf spiral and LSB galaxies, with preference for the currently favoured  $\Lambda$ CDM model [7] (Fig. 5(a)).

(2) The TIS+PS model also predicts the correlations of central mass and phase-space densities,  $\rho_0$  and  $Q \equiv \rho_0/\sigma_V^3$ , of dark matter halos with their velocity dispersions  $\sigma_V$ , with data for low-redshift dwarf spheroidals to X-ray clusters again most consistent with  $\Lambda$ CDM [22] (Fig. 5 (b,c)). There have been recent claims that  $\rho_0 = \text{const}$  for all cosmological halos, independent of their mass, as expected for certain types of SIDM [5,11]. This claim, however does not seem to be supported by most current data (Fig. 5 (c)).

This work was supported by European Community RTN contract HPRN-CT2000-00126 RG29185, grants NASA NAG5-10825 and TARP 3658-0624-1999.

## References

1. Binney, J., & Tremaine, S.: *Galactic Dynamics* (Princeton University Press, Princeton 1987)
2. Burkert, A.: ApJ, **447**, L25 (1995)

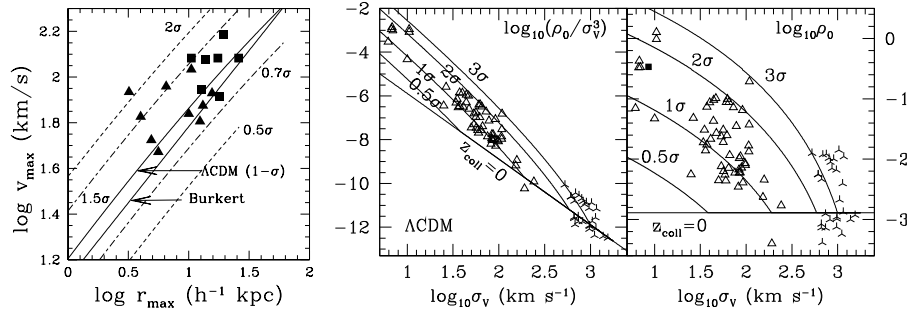


**Fig. 5.** Correlations predicted by (TIS+PS) model for  $\Lambda$ CDM [COBE normalized,  $\Omega_0 = 1 - \lambda_0 = 0.3$ ,  $h = 0.65$ ; no tilt], for halos formed from  $\nu - \sigma$  fluctuations [i.e.  $\nu \equiv \delta_{\text{crit}}(z)/\sigma(M, z)$ ,  $\sigma(M, z) =$  standard deviation of linear density fluctuations filtered on mass scale  $M$ ; typical  $M(z_{\text{coll}}) = M(\nu = 1)$ ], as labelled with  $\nu$ -values. All curves are (TIS+PS) results, except curve in (a) labelled “Burkert” is a fit to data [2]. (a) (left)  $v_{\max} - r_{\max}$  correlation. Observed dwarf galaxies (triangles) and LSB galaxies (squares) from [14]; (b) (middle)  $Q - \sigma_v$  correlation. Line representing halos of different mass which collapse at the same redshift is shown for the case  $z_{\text{coll}} = 0$ . Data points for galaxies and clusters are from the following: (1) 49 late-type spirals of type Sc-Im and 7 dSph galaxies from [12,13] (open triangles); (2) Local Group dSph Leo I from [15] (filled square); (3) 28 nearby clusters,  $\sigma_v$  from [6] and [9], and  $\rho_0$  from [17] (crosses). (c) (right) Same as (b), except for  $\rho_0$  vs.  $\sigma_v$ .

3. Dressler, A., & Smail, I., Poggianti, B.M., Butcher, H., Couch, W.J., Ellis, R.S., Oemler, A., Jr.: APJS, **122**, 51 (1999)
4. Evrard, A.E., Metzler, C.A., & Navarro, J.F.: ApJ, **469**, 494 (1996)
5. Firmani, C., D’Onghia, E., Chincarini, G., Hernandes, X., & Avila-Reese, V.: MNRAS, **321**, 713 (2000)
6. Girardi, M., Giuricin, G., Mardirossian, F., Mezzetti, M., Boschin, W.: ApJ, **505**, 74 (1998)
7. Iliev, I.T. & Shapiro, P.R.: ApJ, **546**, L5 (2001a)
8. Iliev, I.T., & Shapiro, P.R.: MNRAS, **325**, 468 (2001b) (Paper II)
9. Jones, C. & Forman, W.: ApJ, **511**, 65 (1999)
10. Jang-Condell, H., & Hernquist: ApJ, 548, 68 (2001)
11. Kaplinghat, M., Knox, L., & Turner, M.S.: Phys.Rev.Lett., **85**, 3335 (2000)
12. Kormendy, J. & Freeman, K. C.: ‘Scaling laws for dark matter halos in late-type and dwarf spheroidal galaxies’. In *Ringberg Proceedings 1996 Workshop*, eds. R. Bender, T. Buchert, P. Schneider, & F. von Feilitzsch (MPI, Munich 1996), pp. 13 - 15
13. Kormendy, J. & Freeman K.C. 2001, in preparation
14. Kravtsov, A.V., Klypin, A.A., Bullock, J.S., & Primack, J.R.: ApJ, **502**, 48 (1998)
15. Mateo, M., Olszewski, E.W., Vogt, S.S., & Keane, M.J.: ApJ, **116**, 2315 (1998)
16. Mathiesen, B.F., & Evrard A.E.: ApJ, **546**, 100 (2001)
17. Mohr, J.J., Mathiesen, B.F., & Evrard A.E.: ApJ, **517**, 627 (1999)
18. Navarro, J., Frenk, C. S., White, S. D. M.: ApJ, **462**, 563 (1996)
19. Press, W.H., & Schechter, P.: ApJ, **187**, 425 (1974)
20. Shapiro P.R.: ‘Cosmological Reionization’. In: Proceedings of the 20th Texas Symposium on Relativistic Astrophysics and Cosmology, eds. H. Martel and J. C. Wheeler, (AIP Conference Series, v.586, 2001), pp. 219-232

21. Shapiro, P.R., & Iliev, I.T.: ApJ, **542**, L1 (2001)
22. Shapiro, P.R., & Iliev, I.T.: ApJL, accepted (2002) (astro-ph/0107442)
23. Shapiro, P.R., Iliev, I.T., & Raga, A.C.: MNRAS, **307**, 203 (1999) (Paper I)
24. Tyson J.A., Kochanski, G.P., and Dell'Antonio I.P.: ApJ, **498**, L107 (1998)